Structural and Functional Glycosphingolipidomics by Glycoblotting with an Aminooxy-Functionalized Gold Nanoparticle[†]

Noriko Nagahori,[‡] Midori Abe,[‡] and Shin-Ichiro Nishimura*[,‡,§]

Laboratory for Advanced Chemical Biology, Graduate School of Advanced Life Science, and Frontier Research Center for the Post-Genome Science and Technology, Hokkaido University, N21, W11, Sapporo 001-0021, Japan, and Drug-Seeds Discovery Research Laboratory, National Institute of Advanced Industrial Science and Technology (AIST), Sapporo 062-8517, Japan

Received August 28, 2008; Revised Manuscript Received December 9, 2008

ABSTRACT: Glycosphingolipids (GSLs) synthesized in Golgi apparatus by sequential transfer of sugar residues to a ceramide lipid anchor are ubiquitously distributing on vertebrate plasma membranes. A standardized method allowing for high-throughput structural profiling and functional characterization of living cell surface GSLs is of growing importance because they function as crucial signal transduction molecules in various processes of dynamic cellular recognitions. However, methods are not available for amplification of GSLs, while the genomic scale PCR amplification permits large-scale mammalian proteomic analysis. Here we communicate such an approach to a novel "omics", namely, glycosphingolipidomics based on the "glycoblotting" method. The method, which involves selective ozonolysis of the C−C double bond in the ceramide moiety and subsequent enrichment of generated GSL aldehydes by chemical ligation using an aminooxy-functionalized gold nanoparticle (aoGNP) should be of widespread utility for identifying and characterizing whole GSLs present in the living cell surfaces. The present protocol using glycoblotting permitted MALDI-TOFMS-based high-throughput structural profiling of mouse brain gangliosides such as GM1, GD1a/GD1b, and GT1b for adult or GD3 in the case for the embryonic mouse. When mouse melanoma B16 cells were subjected to this protocol, it was demonstrated that gangliosides enriched from the plasma membranes are the only GM3 bearing microheteogeneity in the structure of the *N*-acyl chain. Surface plasmon resonance analysis revealed that aoGNP displaying whole GSLs blotted from mouse B16 melanoma cell surfaces can be used directly for monitoring the specific interaction with the self-assembled monolayer (SAM) of Gg3Cer (gangliotriaosylceramide). Our results indicate that GSL-selective enrichment onto aoGNP from living cell surfaces allows for rapid reconstruction of plasma membrane models mimicking the intact GSL microdomain feasible for further structural and functional characterization.

Since cell surface GSLs[1] and their sialic acid-containing derivatives, gangliosides, exhibit various and crucial functions in cell growth, differentiation, adhesion, recognition, and malignant alteration, there has been of growing attention toward structural and functional analysis of living cell surface GSLs (*1*). It has been documented that dramatic changes in GSL composition and metabolism are strongly associated with oncogenic transformation (*2, 3*). Therefore, identification of disease-related structural alteration of cell surface GSLs will become a key to develop diagnostic biomarkers and therapeutic anticancer vaccines. However, purification and structural characterization of relatively low abundance GSLs have not been routinely possible to date, typically requiring tedious and time-consuming extraction/purification steps of GSLs of interest from extremely complex mixtures before analysis. In general, protocols for the isolation of GSLs would vary depending upon the analytical methods as well as chemical properties of individual GSLs and would need specialized expertise at step-by-step/case-by-case handling for separation. These crucial problems in the enrichment of whole GSLs make it difficult to achieve high-throughput structural and functional analyses of biologically important GSLs. In addition, we should pay attention to the fact that cell surface GSLs often exhibit specific biological functions through specific and dynamic mechanisms such as clustering or self-assembling in order to enhance the strength in the interaction with partner molecules. For example, it was suggested that tumor-associated GSLs are locating at high

[†] This work is supported by a grant for "Innovation COE program for future drug discovery and medical care" from the Ministry of Education, Culture, Science, and Technology of Japan.

* To whom correspondence should be addressed. E-mail: shin@glyco.sci.hokudai.ac.jp. Phone: +81-11-706-9043. Fax: +81-11-706-9042.

[‡] Hokkaido University.

[§] National Institute of Advanced Industrial Science and Technology.

[1] Abbreviations: GSLs, glycosphingolipids; aoGNP, aminooxy-functionalized gold nanoparticle; MALDI-TOFMS, matrix-assisted laser desorption ionization time-of-flight mass spectrometry; SAM, self-assembled monolayer; GNP, gold nanoparticle; Boc, *N-tert*-butoxycarbonyl; TEM, transmission electron microscope; HPAE-PAD, high-pH anion-exchange column chromatography with pulsed amperometric detection. Abbreviations of GSLs are as follows: GM1a, Galβ1−3GalNAcβ1−4(NeuAcα2−3)Galβ1−4Glcβ-Cer; GD1a, NeuAcα2−3Galβ1−3GalNAcβ1−4(NeuAcα2−3)Galβ1−4Glcβ-Cer; GD1b, Galβ1−3GalNAcβ1−4(NeuAcα2−8NeuAcα2−3)Galβ1−4Glcβ-Cer; GT1b, NeuAcα2−3Galβ1−3GalNAcβ1−4(NeuAcα2−8NeuAcα2−3)Galβ1−4Glcβ-Cer; GD3,NeuAcα2−8NeuAcα2−3Galβ1−4Glcβ- Cer; GM3, NeuAcα2−3Galβ1−4Glcβ-Cer; Gg3, GalNAcβ1−4Galβ1−4Glcβ-Cer.

10.1021/bi801640n CCC: $40.75
Published on Web 12/31/2008

density in tumor cells and may be organized in microdomains at the tumor cell surface (*4, 5*). It seems likely that the presence of such microdomains is of fundamental importance for the investigation of dynamic function of GSLs as tumor antigens, adhesion molecules, and signaling molecules, because formation of the microdomain by clustering of GSLs might become an essential mechanism to serve their immunogenicity and antigenicity (*1*). Therefore, we thought that a novel strategy allowing both for structural profiling and for functional analysis of GSLs as the major component of the cell surface microdomain is now strongly expected.

We have demonstrated the versatility of chemical ligation of reactive carbonyl groups by means of aminooxy- or hydrazine-functionalized polymers in selective enrichment analysis of whole *N*-glycans (*6*−*12*) and some kinds of glycopeptides (*8, 13*) derived from serum, cellular glycoproteins, and biopharmaceuticals. The new concept of "glycoblotting", a glycan enrichment technology based on the above chemical ligation, greatly facilitated further quantitative and large-scale glycomics and glycoproteomics using general mass spectrometry-based analyses for the purpose of exploring clinically potential biomarkers (*11*−*13*).

On the other hand, it is well-known that metal and semiconducting nanoparticles are nice tools of the scaffold materials displaying various biomolecules through the specific Au−S bonding (*14*). Since these nanoparticles conjugated with biomolecules are soluble or well dispersed in aqueous solution and stable under physiological conditions, they have been widely applied in broad scientific fields of biochemistry and chemical biology for the molecular recognition assay (*15*−*18*). Metal nanoparticles have also been used as a matrix for LDI-MS analysis, where the metal particles serve as a reservoir for photon energy deposition (*19, 20*). Advantages of the use of a gold nanoparticle (GNP) in MALDI-TOFMS-based structural characterization may be summarized as follows: (a) GNP exhibits much greater ionization efficiency than common organic matrices due to the quantum coefficient effect (*21*), (b) the self-assembled monolayer (SAM) of the thiol compound chemisorbed onto the Au surface can be ionized efficiently to cleave the Au−S bond by laser irradiation in the MALDI process (*22*), and (c) conjugating mass-limited small molecules onto the colloidal Au surface makes it possible to sequester and transfer small quantities of analytes with high efficiency (*23*). Recently, our results revealed that ionization of analytes is highly enhanced by specific laser scattering or diffused reflection on the extremely increased surface area of metal nanoparticles (*24*), which may greatly accelerate the ionization of chemisorbed small molecules from GNP (*24, 25*).

We hypothesized that a streamlined protocol by integrating the above two technologies, "glycoblotting and GNP-assisted MALDI-TOFMS", makes an enrichment analysis of living cell surface glycosphingolipids possible. Here we communicate for the first time a comprehensive approach of structural and functional glycosphingolipidomics based on the glycoblotting method.

EXPERIMENTAL PROCEDURES

General Methods and Materials. If not mentioned, all reagents were used without further purification. *N-tert*-Butoxycarbonyl- (Boc-) aminooxyacetic acid and ganglio-sides (bovine brain) were purchased from EMD Chemicals Inc. (Germany). GalCer (bovine spinal cord), LacCer, and Gg3 (bovine brain) were obtained from Wako Pure Chemical Industries, Ltd. (Japan). Mice were purchased from CLEA JAPAN, Inc. NMR spectra were recorded and measured on AVANCE 600 (Bruker, Germany). All mass measurements were performed using an Ultraflex TOF/TOF mass spectrometer (Bruker Daltonics GmbsH, Bremen, Germany) equipped with a reflector and controlled by the Flexcontrol 1.2 software package. Ions generated by a pulsed UV laser beam (nitrogen laser, $\lambda = 337$ nm) were accelerated to a kinetic energy of 23.5 kV. External calibration of MALDI mass spectra was carried out using singly charged monoisotopic peaks of a mixture of human angiotensin II (*m*/*z* 1046.542), bombesin (*m*/*z* 1619.823), ACTH (*m*/*z* 2465.199), and somatostain 28 (*m*/*z* 3147.472). The mixture of these peptides was measured on the central spot of a 3 × 3 square with external calibration. To achieve mass accuracy better than 60 ppm, internal calibration was carried out by doping the matrix solution with a mixture of the calibration peptides. Calibration of these mass spectra was performed automatically utilizing a customized macro command of the XMASS 5.1.2 NT software package. The macro command was used for the calibration of the monoisotopic singly charged peaks of the above-mentioned peptides. All of the data processing and calculations were performed by Mictosoft Excel and Graphpad Prism. FAB-MS analysis was performed on JMS-HX110 (JEOL, Japan). TEM image was obtained by using JEM-2000FX (200 kV; JEOL, Japan). Ozonolysis was carried out by means of ozone generator NG-N-O_3 (Yodogawarikakogyo, Japan). HPAE-PAD analysis was performed on Dionex Bio LC equipped with a carbopack PA-1 column and pulsed amperometric detector (PAD-II) (Sunnyvale, CA). The LB membrane was prepared using LB LIFT Controller (FSD-21) and FILM BALANCE Controller FSD-300 (USI, Japan). SPR measurements were performed using Biacore 2000 (Biacore AB, Uppsala, Sweden).

*Synthesis of Functional Linkers. 12-N-(tert-Butoxycarbonyl)aminohexa(ethylene glycol) (***6***).* To a solution of compound **5** (480 mg, 1.70 mmol) in methanol (10 mL) were added di-*tert*-butyl dicarbonate (470 μL, 2.05 mmol) and 1 M NaOH(aq) (1 mL). The mixture was stirred for 15 min at 0 °C and for 1 h at room temperature. Then, the mixture was concentrated, and the residue was purified by silica gel column chromatography (50:1 CH_2Cl_2/MeOH) to give compound **6** as a clear oil (455 mg, 70%). ^{1}H NMR (600 MHz, $CDCl_3$) δ 5.22 (s, 1 H, −NH−), 3.76−3.53 (m, 22 H, $-OCH_2-CH_2-O-$), 3.31 (m, 2 H, $-NHCH_2-$), and 1.44 (s, 9 H, *tert*-butyl).

*Undec-1-en-11-yl-12-(N-tert-butoxycarbonyl)aminohexa-(ethylene glycol) (***7***).* Sodium hydride (85 mg, 2.13 mmol) was added to a solution of compound **6** (393 mg, 1.03 mmol) in dry THF (10 mL) under a nitrogen atmosphere at 0 °C. After 15 min, 11-bromo-1-undecene (670 μL, 3.10 mmol) was added to the mixture, and the mixture was stirred for 5 h under a nitrogen atmosphere at room temperature. The reaction was quenched by addition of methanol, and the mixture was filtered. The filtrate was concentrated, and the residue was subjected to purification by silica gel column chromatography (100:1 CH_2Cl_2/MeOH) to afford **7** (357 mg, 65%). ^{1}H NMR (600 MHz, $CDCl_3$) δ 5.84 (m, 1 H, *HC*═), 5.05, (s, 1 H, −CO−N*H*−), 5.00−4.91 (dd, 2 H, $J = 16.8$,

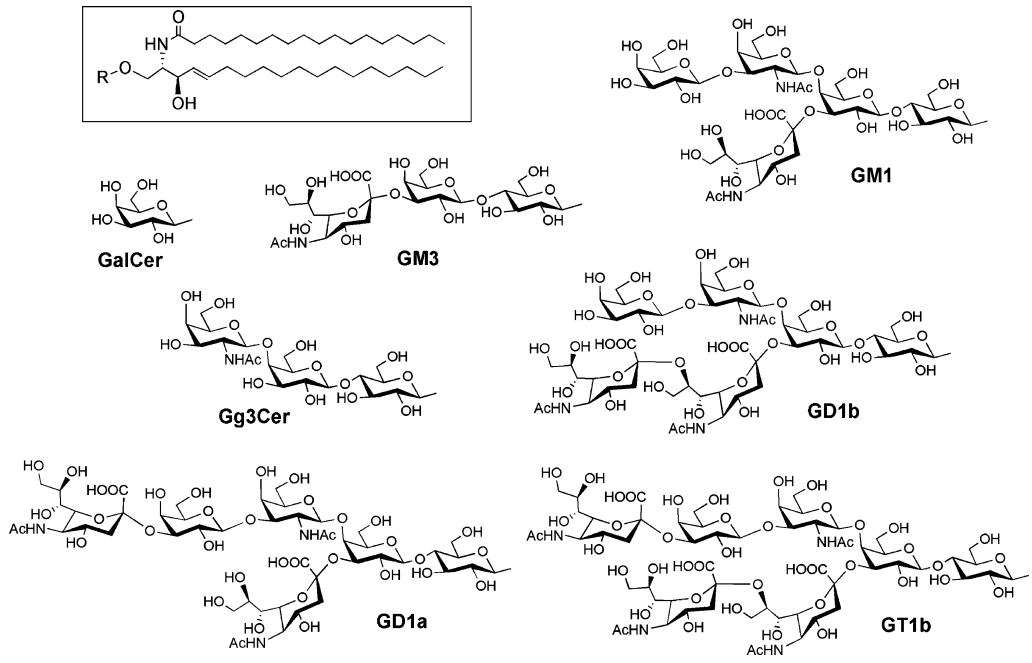

FIGURE 1: Chemical structures of major glycosphingolipids used in this study.

1.2 Hz/10.2, 0.60 Hz, $=CH_2$), 3.65−3.56 (m, 20 H, $-OCH_2-CH_2-O-$), 3.53 (t, 2 H, J = 7.20 Hz, $-NHCH_2CH_2O-$), 3.44 (t, 2 H, J = 6.60, $-OCH_2-$), 3.31 (m, 2 H, $-NH-CH_2-$), 2.04 (q, 2 H, J = 6.60 Hz, $-CH_2-CH=$), 1.57 (q, 2 H, J = 7.20 Hz, $O-CH_2-CH_2$), 1.44 (s, 9 H, *tert*-butyl), and 1.38−1.28 (m, 12 H, $-CH_2-$).

*1-Thioacetylundec-11-yl-12-N-(tert-butoxycarbonyl)aminohexa(ethylene glycol) (***8***).* Thioacetic acid (282 μL, 3.75 mmol) and 2,2′-azobis(isobutyronitrile) (21.5 mg, 0.15 mmol) weres added to a solution of compound **7** (200 mg, 0.375 mmol) in dry THF (5 mL). The reaction mixture was irradiated in a photochemical reactor (UV, 254 nm) under a nitrogen atmosphere at 60 °C. After 12 h, the reaction mixture was concentrated, and the residual syrup was subjected to purification by silica gel column chromatography (100:1 CH_2Cl_2/MeOH) to give **8** as a clear oil (212 mg, 93%). ^{1}H NMR (600 MHz, $CDCl_3$) δ 5.06 (s, 1 H, $-CO-NH-$), 3.65−3.57 (m, 20 H, $-OCH_2-CH_2-O-$), 3.53 (m, 2 H, $-NH-CH_2-CH_2-O-$), 3.44 (t, 2 H, J = 6.60 Hz, $-O-CH_2-$), 3.31 (br, 2 H, $-NH-CH_2-$), 2.87 (t, 2 H, J = 7.20, $-CH_2-S-$), 2.319 (s, 3 H, SAc), 1.58−1.533 (m, 4 H, $-CH_2-CH_2-S-$ and $-CH_2-CH_2-O-$), 1.44 (s, 9 H, *tert*-butyl), and 1.36−1.26 (m, 12 H, $-CH_2-$).

*11,11′-Dithiobis[(undec-11-yl)-12-aminohexa(ethylene glycol)] (***9***).* Sodium methoxide (20.5 mg, 0.373 mmol) was added to a solution of compound **8** (190 mg, 0.312 mmol) in methanol (5 mL) and stirred for 1 day at 0 °C. The reaction mixture was neutralized with Dowex 50W-X8 (H^+), and the resin was filtered. The filtrate was concentrated to give an oily intermediate, 11,11′-dithiobis[undec-11-yl-12-*N*-(*tert*-butoxycarbonyl)aminohexa(ethylene glycol)], in quantitative yield (176 mg). A part of the above intermediate (80 mg, 0.0706 mmol) in 20% trifluoroacetic acid−CH_2Cl_2 (1 mL) was stirred at room temperature for 1 h. The reaction mixture was concentrated, and the residual syrup was purified by silica gel column chromatography (20:1 CH_2Cl_2/MeOH) to give compound **9** as a clear oil (73 mg, 91%). ^{1}H NMR (600 MHz, $CDCl_3$) δ 8.11 (s, 4 H, NH_2-), 3.83 (t, 4 H, J = 4.8, $-NH_2-CH_2-CH_2-O-$), 3.73−3.56 (m, 40 H, $-O-CH_2-CH_2-O-$), 3.43 (t, 2 H, J = 6.60, $-O-CH_2-$), 3.17 (br, 4 H, $-NH_2-CH_2-$), 2.68 (t, 4 H, J = 7.20, $-CH_2-S-$), 1.67 (q, 4 H, J = 7.20, $-CH_2-CH_2-S-$), 1.56−1.53 (br, 4 H, $-CH_2-CH_2-O-$), 1.40−1.35 (br, 4 H, $-CH_2-CH_2-CH_2-S-$), and 1.27 (br, 24 H, $-CH_2-$).

*11,11′-Dithiobis[undec-11-yl-12-{(N-tert-butoxycarbonyl)aminooxyacetyl}aminohexa(ethylene glycol)] (***1***).* To a solution of **9** (18 mg, 19.3 μmol) and (*N*-*tert*-butoxycarbonyl)aminooxyacetic acid (18.5 mg, 96.5 μmol) in chloroform−methanol (1:1, 5 mL) was added *N*,*N*-diisopropylethylamine (17 μL) and 1-(3-dimethylaminopropyl)-3-ethylcarbodiimide hydrochloride (18.5 mg, 96.5 μmol) at 0 °C. The mixture was stirred at room temperature for 21 h. The solvent was removed by evaporation, and the residue was purified by silica gel chromatography (chloroform with methanol gradient from 0 to 2%) to afford **1** (22 mg, 90%). ^{1}H NMR (CD_3OD, 600 MHz) δ 4.33 (s, 4 H, $-NHCO-CH_2-ONHBoc$), 3.78−3.57 (m, 44 H, $-CH_2-O-$), 3.51 (m, 4 H), 3.44 (t, 4 H), 2.68 (t, 4 H, $-CH_2-S-$), 1.66 (m, 4 H, $-CH_2-CH_2-S-$), 1.57 (m, 4 H, $-CH_2-CH_2-CH_2-O-$), 1.48 (s, 18 H, $(CH_3)C-$), and 1.43−1.26 (m, 28 H, $-CH_2-$). MALDI-TOFMS: Calcd for $C_{60}H_{118}N_4O_{20}S_2$ 1278.778, found *m*/*z* 1301.458 $[M + Na]^+$, 1317.474 $[M + K]^+$.

Preparation of Gold Nanoparticles (N-Protected aoGNPs) Displaying Compounds **1** *and* **2**. To a solution of $KAuCl_4$ (70 mg, 1.86 μmol) in Milli-Q water (5 mL) were added compound **1** (13 mg, 1 μmol in 100 μL of 10 mM/MeOH) and compound **2** (760 μg, 1 μmol, 100 μL of 10 mM/Milli-Q water). The solution was gradually added with $NaBH_4$ (100 μL, 100 mM/Milli-Q water) under vigorous stirring, and the mixture became reddish wine color immediately. After being stirred for 3 h, the reaction mixture was subjected to ultrafiltration (Centriplus YM-50, Millipore), and N-protected aoGNPs collected were washed with Milli-Q water five times. The N-protected aoGNPs were suspended in 600 μL of Milli-Q water, and this stock solution was stored at 4 °C in the refrigerator. The solution of N-protected aoGNPs (0.5 μL) was directly subjected to MALDI-TOFMS analysis in

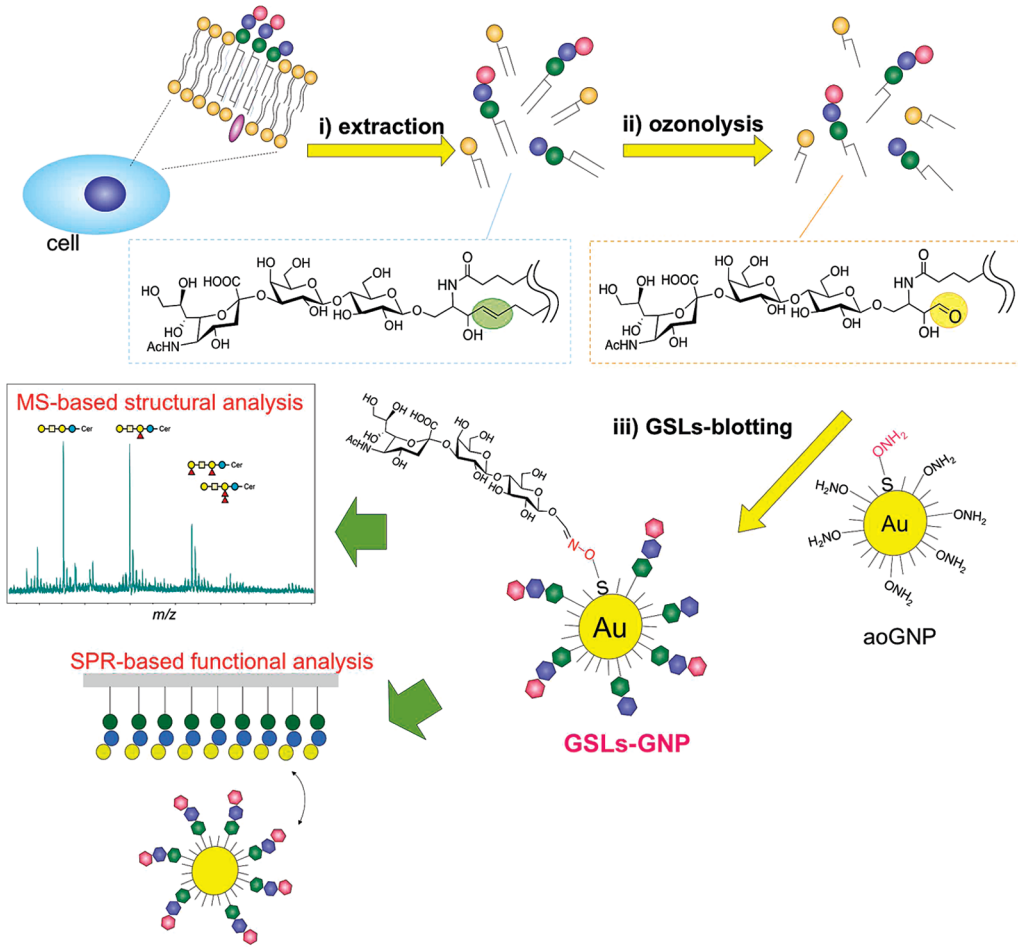

FIGURE 2: A general strategy for structural and functional glycosphingolipidomics based on the selective enrichment of cellular GSLs onto the aoGNP surface by applying the concept of glycoblotting.

the presence of 1 μL of DHB (10 mg/mL) as matrix. Judging from the elemental analysis data (C, 40.14; H, 6.66; N, 1.72), N-protected aoGNPs appear to carry equivalent molar quantities of compounds **1** and **2**. The transmission electron microscopy (TEM) image of N-protected GNPs was measured by JEOL JEM-2000FX, operating at 200 kV. The diameter of GNPs was estimated to be about 1.3 nm, suggesting that a single GNP may be composed of 79 Au atoms and covered by 38 thiol molecules according to the calculation reported by Hosteler et al. (*29*). Thus the N-Boc aminooxyl group on N-protected aoGNPs is calculated to be 0.743 nmol/μL.

Conversion of N-Protected aoGNPs into aoGNPs. Activation (removal of Boc group) of N-protected aoGNPs was performed before use. The mixture of N-protected GNPs (20 μL) [the stock solution of compound **1** (20 μL) should generate 14.9 nmol of aminooxy functional groups] and 2 N HCl(aq) (20 μL) was incubated at 40 °C on the heating block. The reaction mixture was neutralized with 100 mM sodium carbonate, and the aoGNPs were purified by ultracentrifugation using Microcon YM 50 (Millipore). The residual aoGNPs were employed directly for further GSL blotting. MALDI-TOFMS: calcd for the N-deprotected form of **1** (an ion generated from activated aoGNPs, structure "k" listed in Table 1), 1079.6805 $[M + H]^+$; found, 1080.7. Calcd for compound **2** (ions assigned as structures "f" and "g" listed in Table 1), 957.5977 $[M + Na]^+$, 973.5717 $[M + K]^+$; found, 958.4 and 974.4. Calcd for hetero disulfide (ions assigned as structures "h", "i", and "j" listed in Table 1), 1007.6481 $[M + H]^+$, 1029.6301 $[M + Na]^+$, 1045.6040 $[M + K]^+$; found, 1008.5, 1030.6, and 1046.6, respectively.

General Procedure for the Enrichment of GSLs (GSL Blotting) by aoGNPs. (A) Ozonolysis. Using authentic GSLs (commercially available and purified GalCer, LacCer, GM3, and GM1), we established a general procedure for ozonolysis and subsequent enrichment experiments as follows: To a solution of each authentic GSL (200 μM) in chloroform−methanol [1:1 (v/v), 200 μL] was bubbled O_3 gas for 30 min. Then, ozone was removed by N_2 bubbling, and the reaction was quenched by treating with PPh_3 (1 μmol, 1 μL of 1 M solution in toluene). During the O_3 and N_2 bubbling, it was observed that over half amount of the mixed solvent of chloroform−methanol was evaporated. To this mixture was added hexane (500 μL), and the mixture was stirred vigorously. Then, the hexane layer containing simple alkyl aldehyde (byproduct) was removed, and the residue was evaporated to dryness and dissolved in 50 mM sodium acetate buffer (pH 4.0). The solution of each GSL aldehyde was divided into two portions and used for further GSL blotting/MALDI-TOFMS and HPAE-PAD analysis.

(B) GSL Blotting. To the above GSL aldehydes (20 nmol) in sodium acetate buffer (50 mM, pH 4.0) were added the aoGNPs derived from 20 μL (calculated as 14.9 nmol of aminooxy functional groups) of the stock solution of N-protected aoGNPs (**1**) as described above. Then, the mixture was dried by a centrifugal evaporator to complete oximiza-

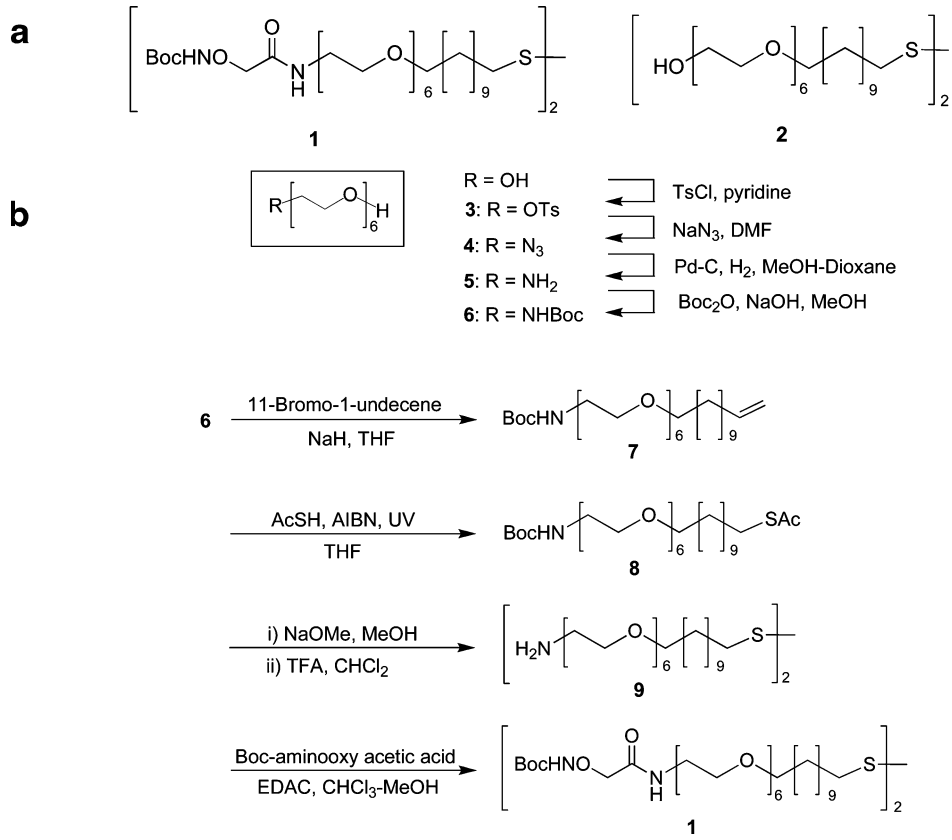

FIGURE 3: Synthesis of key compounds. (a) Chemical structures of functional linkers used in the present study. (b) Synthetic scheme of compound **1**.

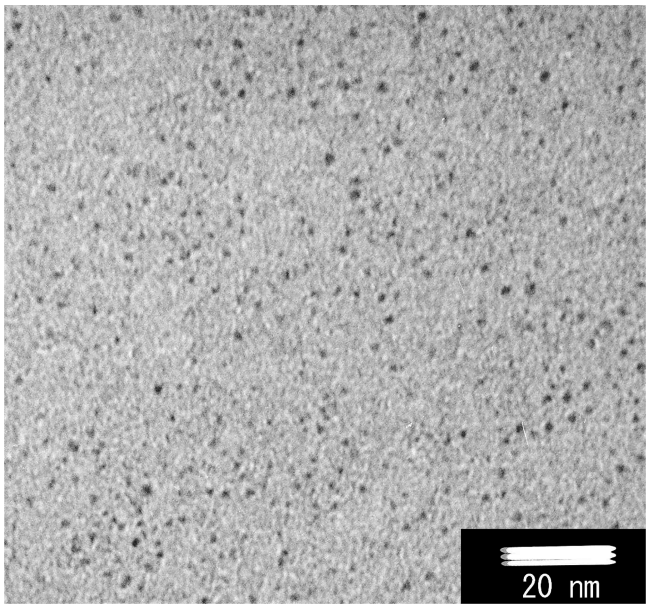

FIGURE 4: TEM view of N-protected aoGNPs.

tion between GSLs and aoGNPs at ambient temperature. The GSLs−GNPs were purified by ultrafiltration (Microcon YM-50; Millipore) and washed thoroughly with Milli-Q water five times. The GSLs−GNPs were suspended in 100 μL of Milli-Q water for storage, and 1 μL of each GSLs−GNPs solution was subjected to MALDI-TOFMS and TOF/TOF analysis in the presence of DHB as matrix (Figure 10). These results clearly indicate that commercially available "purified GSLs" show "microheterogeneity in the structure of *N*-acyl chains as indicated in Figure 10, while glycans can be assigned as expected structures by TOF/TOFMS analysis. Quantitative analysis of enriched GSLs was also carried out by using the HPAE-PAD method to determine individual monosaccharide contents (see Supporting Information). The calibration curve was made by applying authentic GSLs such as GalCer, LacCer, GM3, and GM1 (50 μL, 0.1 mM, 0.5 mM, and 1 mM standard solutions were prepared and used). These authentic GSL solutions and filtrates after "glycoblotting" with aoGNPs were dried by speed vac, and the residues were subjected to hydrolysis by treating with 50% trifluoroacetic acid−water (100 μL). These mixtures were incubated for 1.5 h at 90 °C, Milli-Q water was added (1 mL), and the solutions were lyophilized. The resulting powder was dissolved in 50 μL of Milli-Q water, and each solution (25 μL) was directly injected to HPAE-PAD equipment (100 mM NaOH as eluant) to analyze individual monosaccharide contents. It was revealed that the present protocol using aoGNPs having 14.9 nmol of aminooxy groups (derived from 20 μL of N-protected aoGNP stock solution) allows enrichment of 30% to ~80% of GSLs used [GM1 (5.7 nmol), GM3 (6.5 nmol), LacCer (11.5 nmol), and GalCer (12.5 nmol)], when 20 nmol of standard GSL was employed as described in the above procedure. The results indicate that the single GNP displays 7.3 (GM1), 8.3 (GM3), 14.3 (LacCer), and 16.0 (GalCer) of GSL molecules, respectively. These authentic (well characterized) GSLs−GNPs were used as standard materials for further SPR experiments to determine affinity constants between GSLs enriched from B16 cells and the Gg3 monolayer.

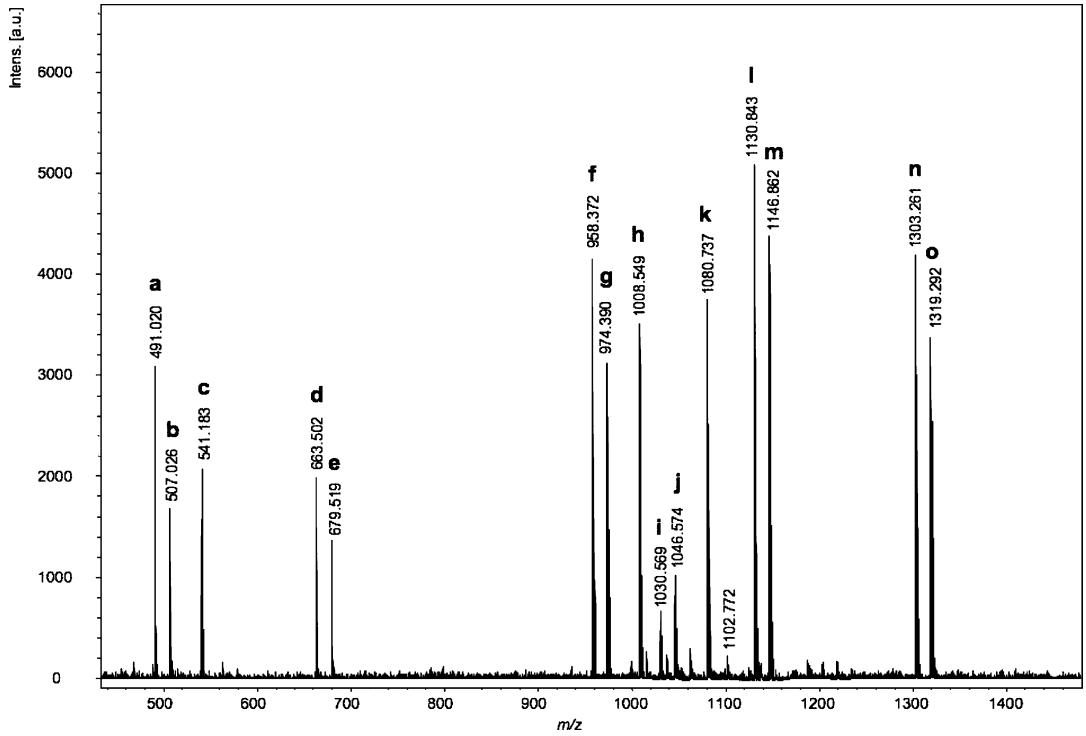

FIGURE 5: Characterization of N-protected aoGNPs by direct MALDI-TOFMS. Chemical formulas of major signals (a−o) detected in this MS are listed in Table 1.

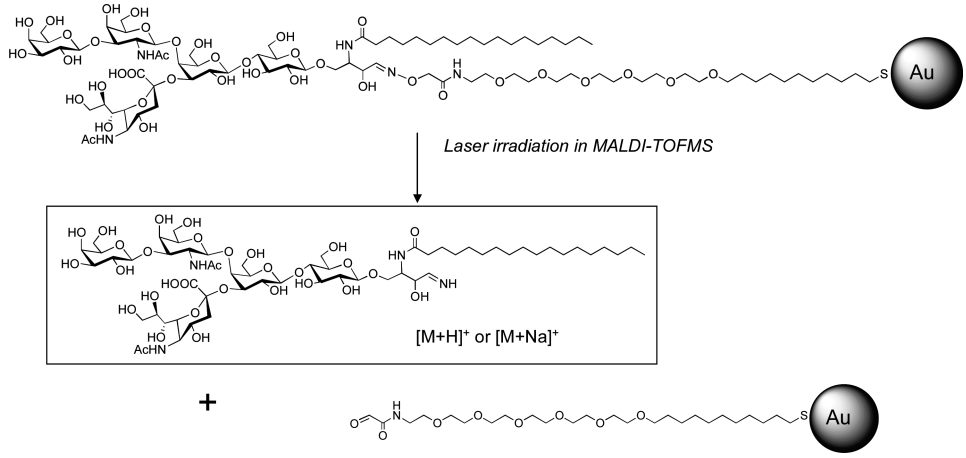

FIGURE 6: Oxime bonds formed between GSL aldehydes and aoGNPs are digested by laser irradiation on the MALDI process to afford highly sensitive imino alcohol ions.

Enrichment of Mouse Brain GSLs. A brain (450 mg, wet weight) from an adult male mouse (C57BL/6JJcl, 7 weeks) and the combined brains of embryos (13.5 days from one female mouse) were homogenized, and the total lipid was extracted with chloroform−methanol (2:1, 1:1, and 1:2). The whole lipid mixture was dried and subjected to the extraction by partition in diisopropyl ether−1-butanol−50 mM NaCl (6:4:5 v/v/v) according to the method reported by Ladisch et al. (*24*). The aqueous layer (10 mL) containing GSLs was collected and stored at 4 °C. The above extract (100 μL, corresponding to 4.5 mg of adult brain) and whole lipid extract in the case of the embryonic brain were subjected to ozonolysis and GSL blotting with aoGNPs (5 μL, ∼3.7 nmol of aminooxy groups) according to the general protocol.

Preparation of aoGNPs Displaying Whole GSLs of B16 Cell Surfaces (Enrichment of Whole GSLs from B16 Melanoma Cells). Preparation of the crude GSL fraction from mouse B16 cells was basically carried out according to the method reported by Hirabayashi et al. (*34*). Mouse B16 cells were incubated in Dulbecco's minimum Eagle's medium supplemented with 10% fetal bovine serum, 10 μg/mL streptomycin, and 10 units/mL penicillin at 37 °C in 5% CO_2. The cells (1.7×10^7) cultivated in eight culture dishes (15 cm) were washed with phosphate buffer (4 mL) four times. To each dish was added the phosphate buffer (2 mL), and the cells were collected using a scraper. The cells were transferred into the four glass centrifuge tubes (∼12 mL), and the tubes were centrifuged at 3000 rpm for 10 min to precipitate the cells. After the supernatant was removed, the mixed solution of chloroform−methanol (9 mL, 1:1 (v/v)) was added and sonicated to homogenize the cells. After incubation at 40 °C for 1 h, the mixture was centrifuged at 3000 rpm for 10 min, and the supernatant was collected. The remaining precipitate was added to chloroform−methanol (9 mL, 2:1 (v/v)), and the mixture was incubated at 40 °C

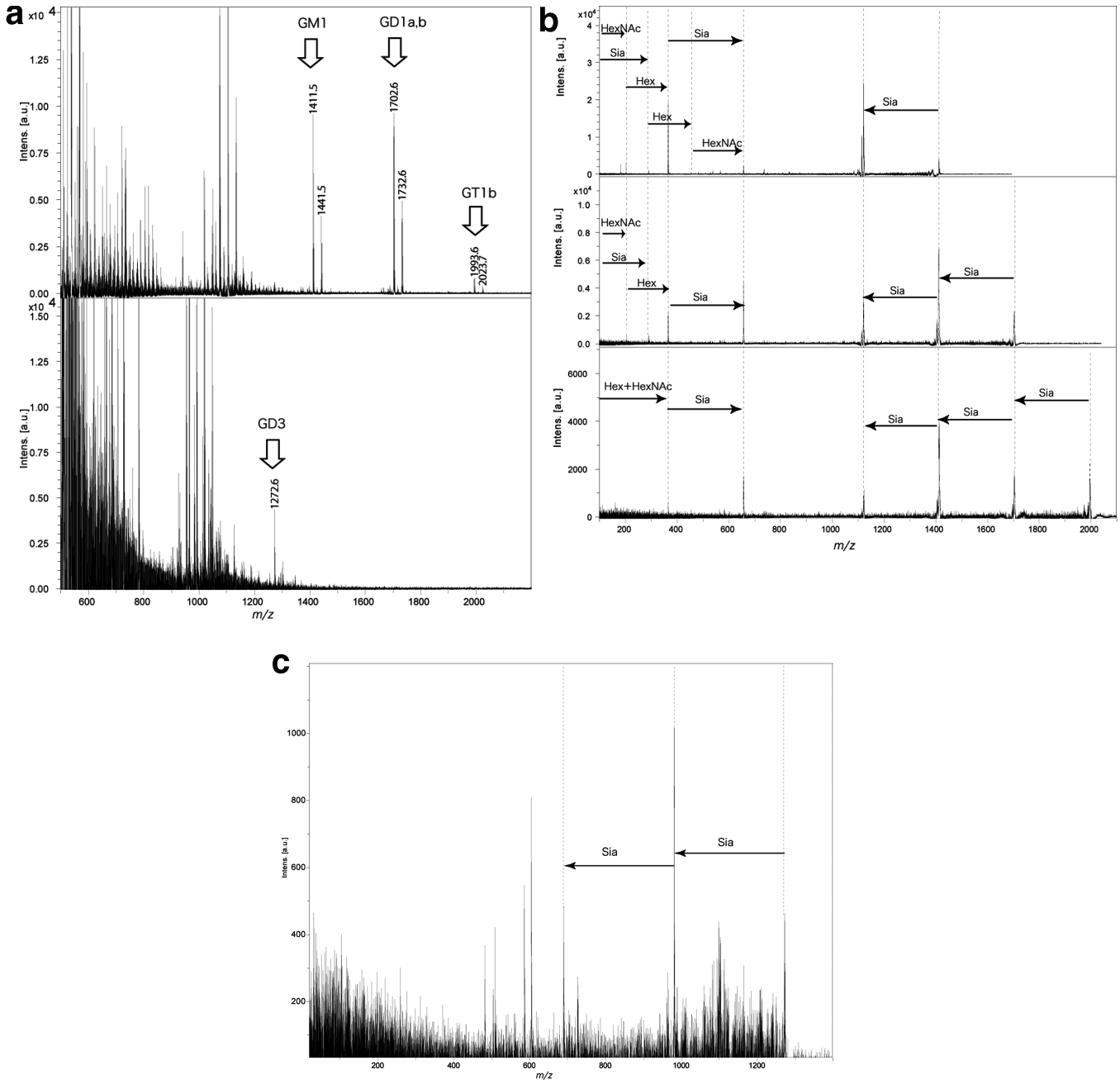

FIGURE 7: Profiling mouse brain glycosphingolipids by glycoblotting and subsequent MALDI-TOFMS. (a) GSLs identified in adult mouse brain (upper panel) and embryonic mouse (bottom panel). (b) MALDI-TOF/TOFMS analysis of the selected peak at *m/z* 1411.5 (GM1), 1702.6 (GD1a/GD1b), and 1993.6 (GT1b) observed in adult mouse brain. (c) MALDI-TOF/TOFMS of a precursor ion at *m/z* 1272.6 corresponding to GD3 detected in embryonic mouse brain.

for 1 h and centrifuged at 3000 rpm for 10 min. Combined supernatants were evaporated to give whole lipid fractions.

The total lipids (isolated from four dishes) dissolved in the mixed solution of butanol−isopropyl ether (6 mL, 1:1 (v/v)) were transferred into the glass centrifuge tube. To this solution was added 50 mM NaCl aqueous solution (3 mL), and the mixture was vigorously stirred using a vortex mixer and centrifuged (1200 rpm for 3 min). After removal of the organic layer, the aqueous layer was mixed with a solution of butanol−isopropyl ether (6 mL, 2:1 (v/v)) and stirred by vortex. Then, the mixture was centrifuged (1200 rpm for 3 min), and the organic layer was removed. The resulted aqueous layer was deposited on a Sep-Pack C18 column (Millipore) and washed with Milli-Q water, eluted by 1:1 (v/v) and 2:1 (v/v) solutions of chloroform−methanol (10 mL) to give crude GSLs. Then, the crude GSLs were dissolved in methanol (200 μL) and employed for the general protocol of ozonolysis and GSL blotting in the presence of aoGNPs (20 μL).

Preparation of Gg3Cer LB Monolayer on SPR Sensor Chip. The solution of Gg3Cer (40 μL, 1 mM solution dissolved in $CHCl_3$/MeOH = 4:1) was developed on the LB trough filled with Milli-Q water. After 15 min, the monolayer was formed by compressing the surface of GSLs to 30 mN/m. The SPR gold sensor chip was vertically dipped into the trough, and the Gg3Cer LB monolayer was transferred onto the SPR sensor chip at a dipping speed of 10 mm/min at 25 °C.

Interaction between GSLs(B16)−GNPs and the Gg3Cer LB Monolayer. The Gg3Cer monolayer was set to the

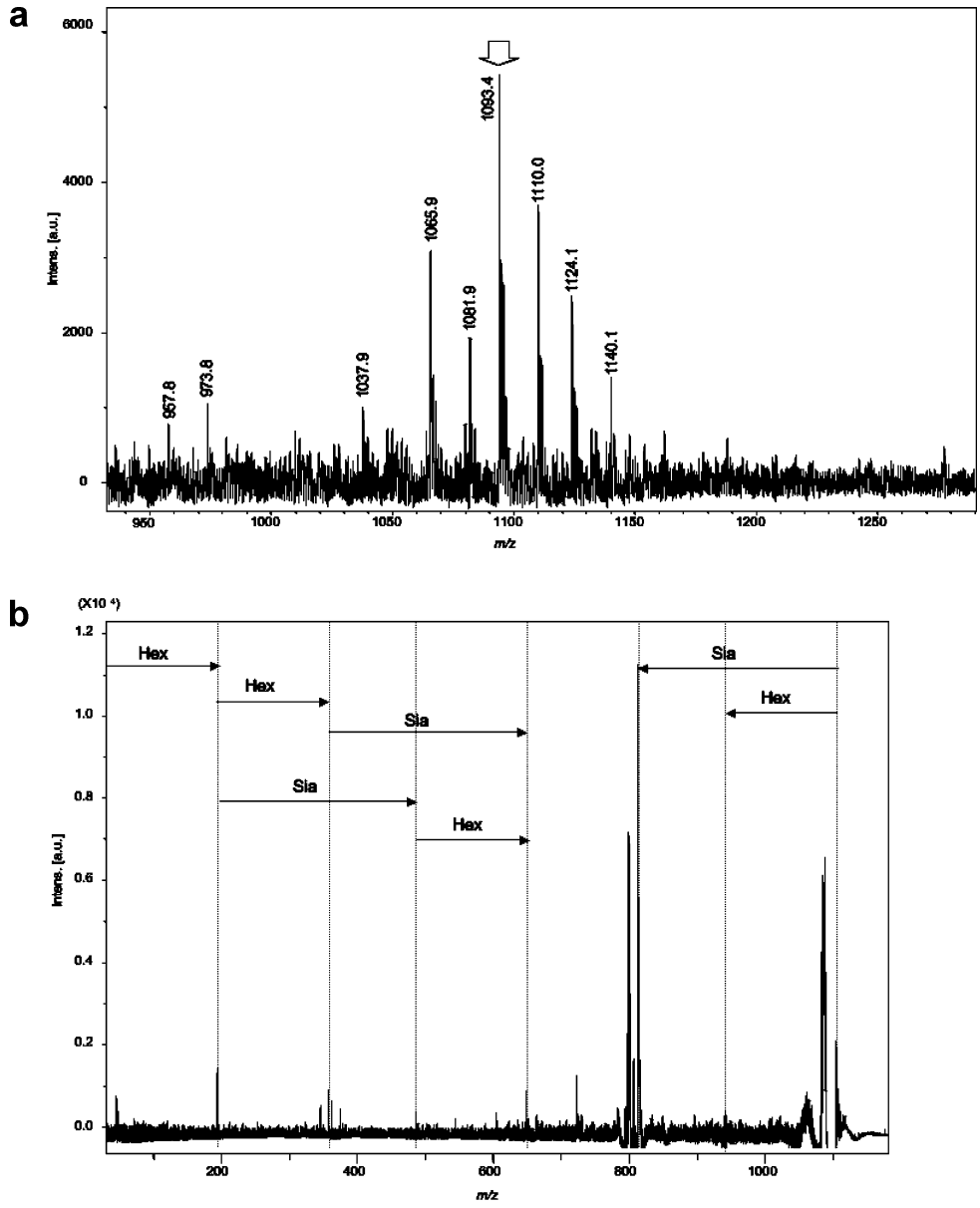

FIGURE 8: Profiling whole GSLs enriched from mouse B16 melanoma cells (C57BL/6). (a) MALDI-TOFMS exhibited multiple ion peaks due to GSL mixture observed in a range from *m/z* 1037.9 to 1140.1. (b) MALDI-TOF/TOFMS of a selected peak at *m/z* 1093.4 revealed that these GSLs are GM3 analogues having various *N*-acyl chains.

instrument and equilibrated with running buffer, and the surface was treated by BSA solution to block nonspecific adsorptions. The solution of GNPs bearing GSLs (50 μL, standard GalCer, LacCer, GM1, GM3, and GSLs enriched from B16 cells in 10 mM HEPES, pH 7.4, 1 mM $CaCl_2$, 0.5 mM $MgCl_2$) was injected to the Gg3Cer LB monolayer immobilized on a sensor chip at the flow rate of 10 μL/min, and the SPR signals were recorded. The concentration of GSLs on aoGNPs injected was determined by HPAE-PAD analysis as described before.

RESULTS AND DISCUSSION

Concept and Preparation of Aminooxy-Functionalized GNPs. Naturally occurring GSLs commonly involve a *trans* double bond at the C-4,5 position of the sphinganine, which can be cleaved quantitatively by simple ozonolysis to generate aldehyde derivatives of the parent GSLs (Figure 1 shows chemical structures of major GSLs used in this study). This characteristic feature of GSLs prompted us to establish a novel and standardized method allowing for structural and functional glycosphingolipidomics concurrently. Figure 2 illustrates a general strategy for the selective enrichment of cellular GSLs onto the GNP surface by applying the concept of glycoblotting, a method based on the chemoselective oxime bond formation between aldehyde and the aminooxy functional group. We devised high-performance and well-dispersed GNP having aminooxy functional groups (aoGNP) by reduction of Au^{3+} ion ($KAuCl_4$) with $NaBH_4$ in the mixed solution of methanol and water in the presence of stabilizing reagents **1** and **2** (Figure 3a). A key compound **1**, an N-protected precursor of the aminooxy-functionalized linker, was synthesized *via* an intermediate **9** derived from hexa(ethylene glycol) as a starting material (Figure 3b). Compound **2**, namely, 1,1′-dithiobis[undec-11-ylhexa(ethylene glycol)] used previously in our report (*24*), was synthesized from hexa(ethylene glycol) according to the previous

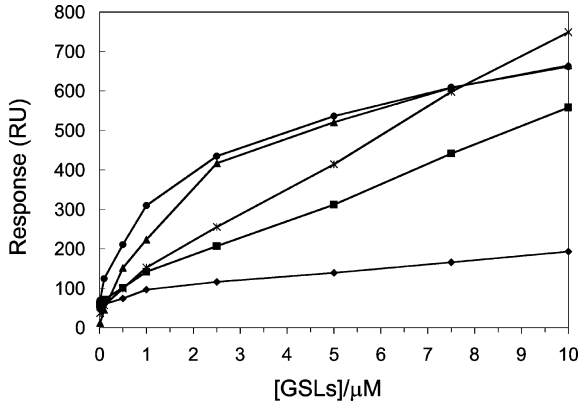

FIGURE 9: SPR analysis of GSL−GSL interaction on the basis of aoGNPs as a platform for displaying high-density GSLs (microdomains). GSLs−GNPs displaying whole GSLs from B16 mouse melanoma cells (●) or purified GSLs such as GalCer (◆), LacCer (■), GM1 (×), and GM3 (▲) were employed as analytes for the SPR-based binding assay with the LB membrane of Gg3Cer.

methods (*15, 18, 24*). Compound **9**, 11,11′-dithiobis[(undec-11-yl)-12-aminohexa(ethylene glycol)] was prepared through *N-tert*-butoxycarbonylated (Boc) derivatives **6**, **7**, and **8** to make rapid and large-scale synthesis of these versatile intermediates and a key compound **1** possible. Compound **5**, 12-aminohexa(ethylene glycol), was synthesized from hexa(ethylene glycol) in three steps (→tosylate **3** (yield 40%) → azide **4** (yield 100%) → amine **5** (yield 100%)). After introduction of *tert*-butoxycarbonyl (Boc) protection at the amino group of compound **5**, alcohol **6** was converted to thioacetate **8** *via* an unsaturated derivative **7**. Removal of *S*-acetyl and *N*-Boc protections by usual conditions afforded the dithio derivative **9** in high yield. Compound **9** was then coupled with *N*-Boc aminooxyacetic acid to afford a precursor **1** in high yield.

The N-protected aoGNPs were prepared by reduction reaction of $KAuCl_4$ in the presence of compounds **1** and **2**. The average diameter of N-protected aoGNP was estimated by TEM view to be 1.3 nm (Figure 4), indicating that single N-protected aoGNP is composed of 79 Au atoms and covered with 38 thiol molecules (*26*−*29*). The MALDI-TOFMS clearly indicate that N-protected aoGNPs are covered by compounds **1** and **2** [signals at *m*/*z* 958.4 (f) and 974.4 (g) correspond to compound **2** and signals at *m*/*z* 1303.3 (n) and 1319.3 (o) are due to compound **1** (Figure 5)]. In addition, the ions observed at *m*/*z* 1008.5 (h), 1030.6 (i), and 1046.6 (j) were assigned as mixed disulfides generated from **1** and **2**. As anticipated, it was also suggested that the urethane-type linkage formed by Boc and aminooxy groups might be degraded under laser irradiation. This characteristic allowed for the liberation of enriched GSLs from aoGNPs through the cleavage of oxime bonds between GSL aldehydes and aminooxy groups of aoGNP to afford highly sensitive imino alcohol ions as illustrated in Figure 6. Proposed chemical formulas of ions generated directly from N-protected aoGNPs by laser irradiation in MALDI-TOFMS are summarized in Table 1.

Structural Glycosphingolipidomics. To illustrate the new method, a crude lipid fraction of C57BL/6JJcl adult (7 weeks) and embryonic (13.5 days) mouse brain extracted by using Ladisch solvent (*30*) [diisopropyl ether−1-butanol−50 mM NaCl(aq) (6:4:5 v/v/v)] was subjected directly to the treatment with O_3 for 30 min and quenched with triphenylphosphine, and the solution containing GSL aldehydes was washed with diisopropyl ether−1-butanol (3:2 v/v) to remove simple alkyl aldehyde as the byproduct. Then, the mixture was allowed to react with aoGNPs. Reaction of GSL aldehydes with aoGNPs proceeded smoothly under mild condition (50 mM sodium acetate buffer, pH 4.0, at ambient temperature) without any special reagent. After evaporating to complete oxime bond formation, GSLs−GNPs were transferred, washed thoroughly by using simple ultrafiltration, and employed directly for subsequent structural characterization. The merit of this method is evident because the whole procedure from GSL enrichment to mass spectrometry-based structural profiling can be performed within ∼3−4 h by employing approximately 100 mg (wet weight) of mouse brain. As anticipated, MALDI-TOFMS showed that aoGNP captures four major gangliosides such as GM1 (*m*/*z* 1411.5 and 1441.5), GD1a/GD1b (*m*/*z* 1702.6 and 1732.6), and GT1b (*m*/*z* 1993.6 and 2003.7) found in general adult mouse brain and GD3 (*m*/*z* 1272.6) found mainly in embryonic mouse brain (Figure 7) (*31*). When GSLs enriched similarly on aoGNP from mouse B16 melanoma cells (1.7×10^7 cells) were subjected to MALDI-TOFMS, multiple ion peaks corresponding to GM3 analogues having various long acyl chains were detected (Figure 8a). This result clearly indicates that the present protocol greatly facilitated analysis of the molecular diversity (microheterogeneity) of GSLs carrying sphingosine with unsaturated lipids in terms of alterations in the *N*-acyl group as well as glycoforms (Figure 8b). Detailed structural analysis of a variety of ceramides including saturated lipids will be possible by reverse glycoblotting based on selective periodate oxidation of neuraminic acids (*13*), which will be reported elsewhere.

Table 1: Proposed Chemical Formulas of Ions Generated from N-Protected aoGNPs

a b	$[M+Na]^+$ $[M+K]^+$	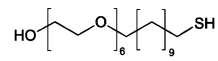
c	$[M+H]^+$	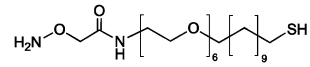
d e	$[M+Na]^+$ $[M+K]^+$	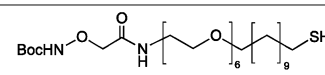
f g	$[M+Na]^+$ $[M+K]^+$	compound 2
h i j	$[M+H]^+$ $[M+Na]^+$ $[M+K]^+$	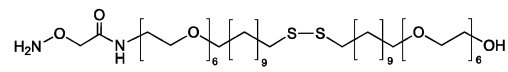
k	$[M+H]^+$	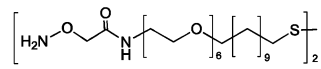
l m	$[M+Na]^+$ $[M+K]^+$	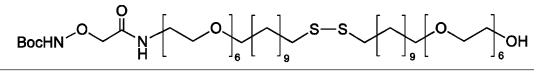
n o	$[M+Na]^+$ $[M+K]^+$	compound 1

Functional Glycosphingolipidomics. Next, our interest was focused on the feasibility of aoGNPs as a tool for the characterization of carbohydrate−carbohydrate interaction conducted by cell surface glycosphingolipids (*32*). It seems that whole GSLs enriched and transferred onto aoGNPs (GSLs−GNPs) from living cell surfaces might become a plausible model of "microdomain" involving high-density

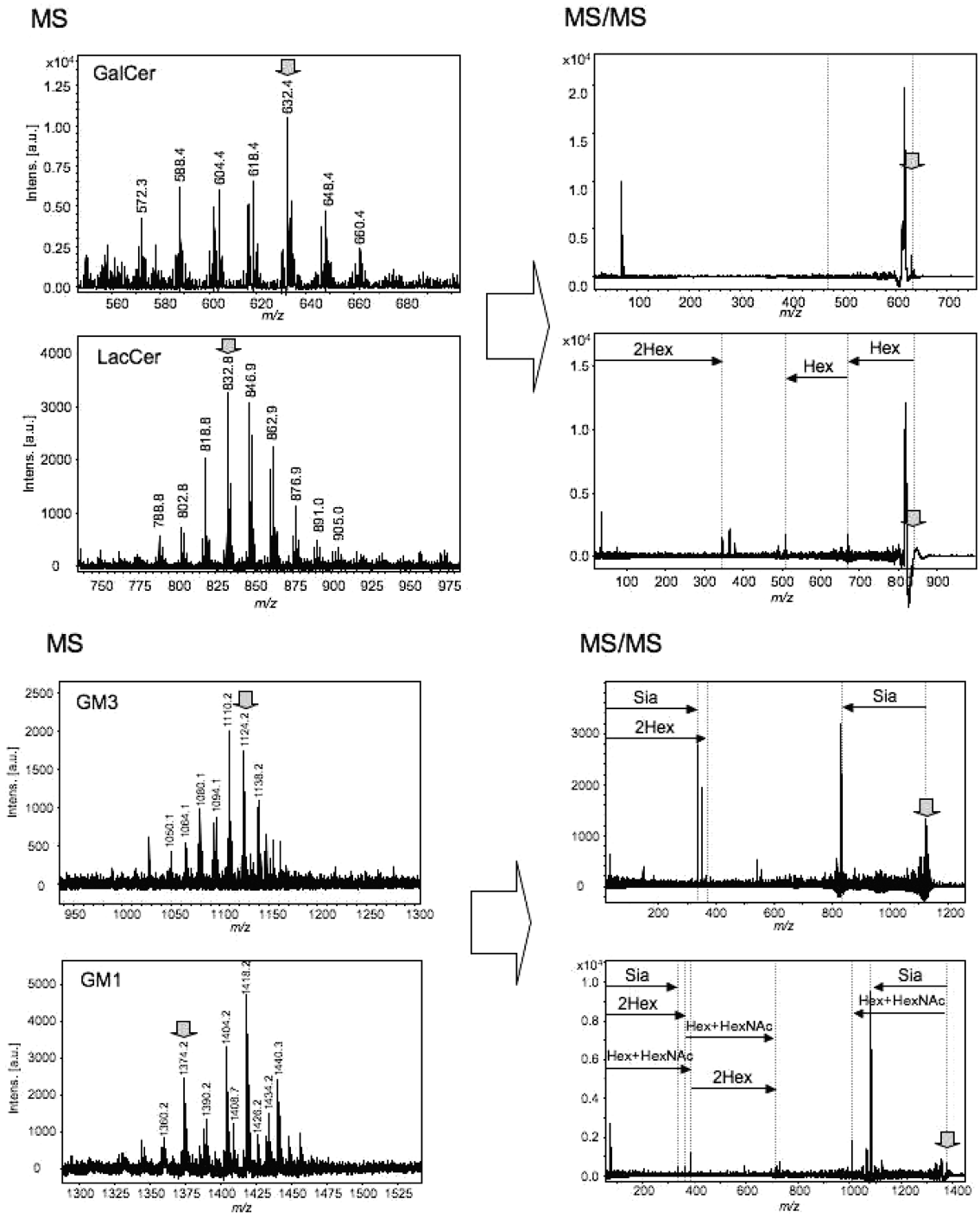

FIGURE 10: MALDI-TOFMS and TOF/TOFMS of enriched GSLs (authentic materials).

GSLs and serves as nice tools for investigating specific functions of self-assembled GSLs under a similar topology to the intact plasma membrane. Here we examined the feasibility of aoGNPs for functional analysis of the above-mentioned B16 cell surface GSLs because it was documented that GM3 is identified as the melanoma-associated antigen in mice, hamsters, and humans (*33*) and microdomain composed of highly expressed GM3 in mouse melanoma B16 cells (*34*) intermediates cancer metastasis through the specific adhesion with Gg3Cer (*35, 36*). In addition to GSLs(B16)−GNPs [whole GSLs on aoGNP enriched from mouse B16 melanoma cells described in the above MS analyses (Figure 8)], we prepared GSLs−GNPs displaying pure GalCer, LacCer, GM1, and GM3 as controls. The calibration curves were also made by using these authentic GSLs−GNPs to determine the amount of total GSLs enriched from B16 cells on the GNPs. The concentration of GSLs−GNPs was estimated by means of pulsed amperometric analysis using high-pH anion-exchange column chromatography (HPAE-PAD) after releasing monosaccharides from GSLs−GNP by acid hydrolysis. The results indicated that approximately 7−16 molecules of GSLs are captured on the surface of the single aoGNP, respectively (the average surface area of the single GNP = 5.3 nm^2). Thus, well-characterized GSLs−GNPs were employed for further binding assay using SPR with the LB membrane of Gg3Cer immobilized on gold substrate. Affinity constants (K_a) were calculated by using a common Langmuir-type equation:

$$[\mathrm{GSLs}]/\Delta\mathrm{RU} = [\mathrm{GSLs}]/\mathrm{RU}_{max} + 1/\mathrm{RU}_{max}K_a$$

Here, ΔRU_{max} means the maximal changes in the SPR upon the injection of the GSLs−GNPs. [GSLs] is the concentration of GSLs−GNPs and is adjusted to be 0.01, 0.1, 0.5, 1.0, 2.5, 5.0, 7.5, and 10 μM. It was revealed that the binding profile of GSLs(B16)−GNPs seems to be quite similar to that of GM3−GNPs, and the affinity constants (K_a) were calculated by applying the above equation to be 4.35×10^5 M^{-1} for GSLs(B16)−GNPs and 3.64×10^5 M^{-1} for GM3−GNPs, respectively (Figure 9). On the other hand, the binding curves of other GSLs−GNPs such as GalCer−GNPs, LacCer−GNPs, and GM1−GNPs did not fit to the above Langmuir-type isothermal adsorption equation at the concentration tested. These results clearly suggest that the binding of GM3−GNPs or GSLs(B16)−GNPs with the Gg3Cer monolayer is a specific and high-affinity interaction (*32*).

In conclusion, we demonstrated that aoGNPs are suitable scaffold material for the high-throughput protocol for the chemical enrichment and subsequent MALDI-TOFMS-based structural characterization of naturally occurring GSLs. It can also be emphasized that use of aoGNPs allows for the reconstruction of the self-assembled microdomain model involving multivalent GSLs and greatly facilitates direct monitoring of the carbohydrate−carbohydrate interaction by means of SPR.

ACKNOWLEDGMENT

We thank Dr. S.-I. Hakomori, Dr. Y. Igarashi, and Dr. Dr. Y. Nagai for stimulating suggestions and discussions.

SUPPORTING INFORMATION AVAILABLE

Additional experimental methods and data. This material is available free of charge via the Internet at http://pubs.acs.org.

REFERENCES

1. Hakomori, S.-I., and Zhang, Y. (1997) Glycosphingolipid antigens and cancer therapy. *Chem. Biol. 4*, 97–104.
2. Hakomori, S.-I. (1996) Tumor malignancy defined by aberrant glycosylation and sphingo(glyco)lipid metabolism. *Cancer Res. 56*, 5309–5318.
3. Hakomori, S.-I., and Murakami, W. T. (1968) Glycolipids of hamster fibroblasts and derived malignant-transformed cell lines. *Proc. Natl. Acad. Sci. U.S.A. 59*, 254–261.
4. Brown, D. A., and London, E. (2000) Structure and function of sphingolipid- and cholesterol-rich membrane rafts. *J. Biol. Chem. 275*, 17221–17224.
5. Hakomori, S.-I. (1990) Bifunctional role of glycosphingolipids. Modulators for transmembrane signaling and mediators for cellular interactions. *J. Biol. Chem. 265*, 18713–18716.
6. Nishimura, S.-I., Niikura, K., Kurogochi, M., Matsushita, T., Fumoto, M., Hinou, H., Kamitani, R., Nakagawa, H., Deguchi, K., Miura, N., Monde, K., and Kondo, H. (2005) High-throughput protein glycomics: combined use of chemoselective glycoblotting and MALDI-TOF/TOF mass spectrometry. *Angew. Chem., Int. Ed. Engl. 44*, 91–96.
7. Niikura, K., Kamitani, R., Kurogochi, M., Uematsu, R., Shinohara, Y., Nakagawa, H., Deguchi, K., Monde, K., Kondo, H., and Nishimura, S.-I. (2005) Versatile glycoblotting nanoparticles for high-throughput protein glycomics. *Chem. Eur. J. 11*, 3825–3834.
8. Shimaoka, H., Kuramoto, H., Furukawa, J., Miura, Y., Kurogochi, M., Kita, Y., Hinou, H., Shinohara, Y., and Nishimura, S.-I. (2007) One-pot solid-phase glycoblotting and probing by transoximization for high-throughput glycomics and glycoproteomics. *Chem. Eur. J. 13*, 1664–1673.
9. Miura, Y., Shinohara, Y., Furukawa, J., Nagahori, N., and Nishimura, S.-I. (2007) Rapid and simple solid-phase esterification of sialic acid residues for quantitative glycomics by mass spectrometry. *Chem. Eur. J. 13*, 4797–4804.
10. Kita, Y., Miura, Y., Furukawa, J., Nakano, M., Shinohara, Y., Ohno, M., Takimoto, A., and Nishimura, S.-I. (2007) Quantitative glycomics of human whole serum glycoproteins based on the standardized protocol for liberating N-glycans. *Mol. Cell. Proteomics 6*, 1437–1445.
11. Furukawa, J., Shinohara, Y., Kuramoto, H., Miura, Y., Shimaoka, H., Kurogochi, M., Nakano, M., and Nishimura, S.-I. (2008) A comprehensive approach to structural and functional glycomics based on chemoselective glycoblotting and sequential tag conversion. *Anal. Chem. 80*, 1094–1101.
12. Miura, Y., Hato, M., Shinohara, Y., Kuramoto, H., Furukawa, J., Kurogochi, M., Shimaoka, H., Tada, M., Nakanishi, K., Ozaki, M., Todo, S., and Nishimura, S.-I. (2008) BlotGlycoABC: An integrated glycoblotting technique for rapid and large-scale clinical glycomics. *Mol. Cell. Proteomics 7*, 370–377.
13. Kurogochi, M., Amano, M., Fumoto, M., Takemoto, A., Kondo, H., and Nishimura, S.-I. (2007) Reverse glycoblotting allows rapid-enrichment glycoproteomics of biopharmaceuticals and disease-related biomarkers. *Angew. Chem., Int. Engl. Ed. 46*, 8808–8813.
14. Katz, E., and Willner, I. (2004) Integrated nanoparticle-biomolecules hybrid systems: synthesis, properties, and applications. *Angew. Chem., Int. Engl. Ed. 43*, 6042–6108.
15. de la Fuente, J. M., Barrientos, A. G., Rojas, T. C., Rojo, J., Canada, J., Fernandez, A., and Penades, S. (2001) Gold nanoparticles as water-soluble polyvalent models to study carbohydrate interactions. *Angew. Chem., Int. Engl. Ed. 40*, 2257–2261.
16. Bruchez, M., Moronne, M., Gin, P., Weiss, S., and Alivisatos, A. P. (1998) Semiconductor nanocrystals as fluorescent biological labels. *Science 281*, 2013–2016.
17. Schofield, C. L., Field, R. A., and Russell, D. A. (2007) Glycon-anoparticles for the colorimetric detection of cholera toxin. *Anal. Chem. 79*, 1356–1361.
18. de la Fuente, J. M., Eaton, P., Barrientos, A. G., Menendez, M., and Penades, S. (2005) Thermodynamic evidence for Ca^{2+}-mediated self-aggregation of Lewis X gold glyconanoparticles. A model for cell adhesion via carbohydrate-carbohydrate interaction. *J. Am. Chem. Soc. 127*, 6192–6197.
19. Tanaka, K., Waki, H., Ido, H., Akita, S., and Yoshida, T. (1988) Protein and polymer analyses up to m/z 100,000 by laser ionization time-of flight mass spectrometry. *Rapid Commun. Mass. Spectrom. 2*, 151–153.
20. Teng, C. H., Ho, K. C., Lin, Y. S., and Chen, Y. C. (2004) Gold nanoparticles as selective and concentrating probes for samples in MALDI MS analysis. *Anal. Chem. 76*, 4337–4342.
21. McLean, J. A., Stumpo, K. A., and Russell, D. H. (2005) Size-selected (2−10 nm) gold nanoparticles for matrix assisted laser desorption ionization of peptides. *J. Am. Chem. Soc. 127*, 5304–5305.
22. Mouradian, S., Nelson, C. M., and Smith, L. M. (1996) A self-assembled matrix monolayer for UV-MALDI mass spectrometry. *J. Am. Chem. Soc. 118*, 8639–8645.
23. Kirk, J. S., and Bohn, P. W. (2004) Surface adsorption and transfer of organomercaptans to colloidal gold and direct identification by matrix assisted laser desorption/ionization mass spectrometry. *J. Am. Chem. Soc. 126*, 5920–5926.
24. Nagahori, N., and Nishimura, S.-I. (2006) Direct and efficient monitoring of glycosyltransferase reactions on gold colloidal nanoparticles by using mass spectrometry. *Chem. Eur. J. 12*, 6478–6485.
25. Su, C.-L., and Tseng, W.-L. (2007) Gold nanoparticles as assisted matrix for determining neutral small carbohydrates through laser desorption/ionization time-of-flight mass spectrometry. *Anal. Chem. 79*, 1626–1633.
26. Biebuyck, H. A., Bain, C. D., and Whitesides, G. M. (1994) Comparison of organic monolayers on polycrystalline gold spontaneously assembled from solutions containing dialkyl disulfides or alkanethiols. *Langmuir 10*, 1825–1831.
27. Badia, A., Demers, L., Dickinson, L., Morin, F. G., Lennox, R. B., and Reven, L. (1997) Gold-sulfur interactions in alkylthiol self-assembled monolayers formed on gold nanoparticles studied by solid-state NMR. *J. Am. Chem. Soc. 119*, 11104–11105.
28. Uyeda, H. T., Medintz, I. L., Jaiswal, J. K., Simon, S. M., and Mattoussi, H. (2005) Synthesis of compact multidentate ligands to prepare stable hydrophilic quantum dot fluorophores. *J. Am. Chem. Soc. 127*, 3870–3878.

29. Hostetler, M. J., Wingate, J. E., Zhong, C.-J., Harris, J. E., Vachet, R. W., Clark, M. R., Londono, J. D., Green, S. J., Stokes, J. J., Wignall, G. D., Glish, G. L., Porter, M. D., Evans, N. D., and Murray, R. W. (1998) Alkanethiolate gold cluster molecules with core diameters from 1.5 to 5.2 nm: Core and monolayer properties as a function of core size. *Langmuir 14*, 17–30.
30. Ladisch, S., and Gillard, B. (1985) A solvent partition method for microscale ganglioside purification. *Anal. Biochem. 146*, 220–231.
31. Ngamukote, S., Yanagishita, M., Ariga, T., Ando, S., and Yu, R. K. (2007) Developmental changes of glycosphingolipids and expression of glycogens in mouse brains. *J. Neurochem. 102*, 2327–2341.
32. Kojima, N., and Hakomori, S.-I. (1989) Specific interaction between gangliotriaosylceramide (Gg3) and sialosyllactosylceramide (GM3) as a basis for specific cellular recognition between lymphoma and melanoma cells. *J. Biol. Chem. 264*, 20159–20162.
33. Nores, G. A., Dohi, T., Taniguchi, M., and Hakomori, S.-I. (1987) Density-dependent recognition of cell surface GM3 by a certain anti-melanoma antibody, and GM3 lactone as a possible immunogen: requirements for tumor-associated antigen and immunogen. *J. Immunol. 139*, 3171–3176.
34. Hirabayashi, Y., Hamaoka, A., Matsumoto, M., Matsubara, T., Tagawa, M., Wakabayashi, S., and Taniguchi, M. (1985) Syngeneic monoclonal antibody against melanoma antigen with interspecies cross-reactivity recognizes GM3, a prominent ganglioside of B16 melanoma. *J. Biol. Chem. 260*, 13328–13333.
35. Otsuji, E., Park, Y. S., Tashiro, K., Kojima, N., Toyokuni, T., and Hakomori, S.-I. (1995) Inhibition of B16 melanoma metastasis by administration of G(M3)- or Gg3-liposomes: Blocking adhesion of melanoma cells to endothelial cells (anti-adhesion therapy) via inhibition of G(M3)-Gg3Cer or G(M3)LacCer interaction. *Int. J. Oncol. 6*, 319–327.
36. Iwabuchi, K., Yamamura, S., Prinetti, A., Handa, K., and Hakomori, S.-I. (1988) GM3-enriched microdomain involved in cell adhesion and signal transduction through carbohydrate-carbohydrate interaction in mouse melanoma B16 cells. *J. Biol. Chem. 273*, 9130–9138.

BI801640N